

Supplementary Information

“Solvothermal growth of a ruthenium metal-organic framework featuring HKUST-1 structure type as thin films on oxide surfaces”

Olesia Kozachuk^a, Kirill Yusenko^a, Heshmat Noei^b, Yuemin Wang^b, Stephan Walleck^c, Thorsten Glaser^c and Roland A. Fischer^{*a}

^a *Inorganic Chemistry II—Organometallics and Materials Chemistry,*

*Ruhr-University Bochum, D-44870 Bochum, Germany. Fax: +49 (0)234 32-14174; Tel: +49 (0)234 32-24174;
E-mail: roland.fischer@rub.de*

^b *Laboratory of Industrial Chemistry, Ruhr-University Bochum, Universitätsstrasse 150, 44801 Bochum, Germany.*

^c *Inorganic Chemistry I, Faculty of Chemistry, Bielefeld University, Universitätsstrasse 25, 33615 Bielefeld, Germany.*

Analytical methods and materials:

For the deposition experiment strips (1.5 cm × 1 cm) of silicon [100] wafer (Wacker Siltronic AG) with a 20 nm layer of SiO₂ and commercial Al₂O₃-coated silicon wafers (Siegert Consulting e.K., Aachen, Germany; thickness of Al₂O₃ – 50 nm) were used. All reagents, except [Ru₂(CH₃COO)₄Cl], were available commercially and utilized without further purification. [Ru₂(CH₃COO)₄Cl] was prepared by using a procedure previously described.¹

Powder X-ray Diffraction (PXRD): PXRD data of Ru-MOF_{as} and deposited oxide samples were collected on an X' Pert PRO PANalytical equipment (Bragg–Brentano geometry with automatic divergence slits, position sensitive detector, continuous mode, room temperature, Cu-K α radiation, Ni-filter, in the range of $2\theta = 5\text{--}50^\circ$, step size 0.01° , time per step – 250 s). For the measurement of Ru-MOF_{ht} a D8-Advance Bruker AXS diffractometer with CuK α radiation ($\lambda = 1.54178 \text{ \AA}$) operating at 25 °C was employed (Göbel mirror; $\theta\text{--}2\theta$ scan; $2\theta = 5\text{--}90^\circ$; step size = $0.0142 (2\theta)$; scan speed = 10 second/step; position sensitive detector; $\alpha\text{-Al}_2\text{O}_3$ as external standard. The sample was filled (glove-box) into standard capillaries (0.7-mm diameter) and measured in Debye-Scherrer geometry.

Scanning Electron Microscopy (SEM): The film morphologies were investigated using a LEO 1530 Gemini Scanning Electron Microscope.

X-ray Photoelectron Spectroscopy (XPS): The XPS measurements were carried out in an ultrahigh vacuum (UHV) setup equipped with a high-resolution Gamdata-Scienta SES 2002 analyzer. A monochromatic Al KR X-ray source (1486.3 eV; anode operating at 14.5 kV and 50 mA) was used as incident radiation. The analyzer slit width was set at 0.3 mm and the pass energy was fixed at 200 eV for all the measurements. The overall energy resolution was better than 0.5 eV. A flood gun was used to compensate for the charging effects. All spectra reported here are calibrated to C 1s core level binding energy at 285 eV. Prior to the elemental scans, a survey scan was measured for all the samples in order to detect all the elements present. The XP spectra were deconvoluted using the CASA XPS program with a Gaussian-Lorentzian mix function and Shirley background subtraction.

Magnetic measurements: Magnetic susceptibility data were measured in the temperature range 2-300 K by using a SQUID magnetometer (Quantum Design MPMS XL-7 EC) with a field of 1.0 T and 0.01 T. VTVH measurements were performed in various static fields (1-7 T) in the range 2-10 K with the magnetization equidistantly sampled on a $1/T$ temperature scale. The experimental data were corrected for underlying diamagnetism by use of tabulated Pascal's constants. The susceptibility data of the dinuclear ruthenium unit were analyzed on the basis of the usual spin-Hamiltonian description for the electronic ground state by using the simulation package julX written by Eckhard Bill for exchange coupled systems.²

The Hamilton operator was:

$$\hat{H} = g\beta \hat{S} \cdot \bar{B} + D[S_z^2 - S(S+1)/3] + E[S_x^2 - S_y^2] \quad (1)$$

where D , E/D are the local axial and rhombic zero field splitting parameters and g is the average electronic g -value. Magnetic moments were obtained from numerically generated derivatives of the eigenvalues of eq. 1, and summed up over 16 field orientations along a 16-point Lebedev grid to account for the powder distribution of the sample.

FTIR-spectra were measured with an ATR setup using a Bruker Alpha FTIR instrument which is placed in a LABStar MB 10 compact MBraun glove-box under argon atmosphere.

UV/VIS spectra were recorded using Lambda 9 Perkin-Elmer UV/VIS Spectrophotometer.

Cyclic and Differential pulse voltammetry was performed using an Autolab PGSTAT12 potentiostat (Eco Chemie, Utrecht, The Netherlands) controlled by GPES 4.7 software (Metrohm, Filderstadt, Germany) in a three-electrode configuration with Ag/AgCl/KCl (3M) reference electrode, a platinum-wire counter electrode and graphite rods were used as working electrodes (type RW001, 3.05 mm diameter, Ringsdorff Werke, Bonn, Germany) sealed in a glass tube using epoxy glue. The electrodes were polished on emery paper (1200) and rinsed with distilled water. All potentials are referred to Ag/AgCl/3 M KCl reference electrode. Ru-MOF_{as} was suspended in ethanolic solution of Nafion (5%) and was deposited on the working electrode. The potential range was from -0.05 to 0.4 V.

N₂ sorption measurements were performed using a Quantachrome Autosorp 1M instrument and optimized protocols.

Thermal gravimetric analysis (TG) of materials was carried out using a Seiko TG/DTA 6300S11 at ambient pressure (sample weight ~ 10 mg, nitrogen gas flow (300 ml min⁻¹), and heating rate – 5°C min⁻¹).

Elemental Analysis for C and H analyses were carried out using a Vario CHNSO EL (1998) instrument.

Film preparation and synthesis of microcrystalline reference sample: Using a custom-made sample holder oxide strips were placed into a mixture of the composition $3\text{RuCl}_3 \times x\text{H}_2\text{O} : 2\text{H}_3\text{btc} : 5\text{CH}_3\text{COOH} : 925\text{H}_2\text{O}$ and it was held at 160°C in a Teflon-lined autoclave for 72 h. After synthesis both substrates were carefully washed several times with water and absolute ethanol, and dried under argon at room temperature. A dark green-grey powder reference sample of Ru-MOF_{as} was collected with a membrane filter as a precipitate at the bottom of the reaction vessel. The crude product was washed with water and dried at room temperature. The calcination of the material was conducted at 100°C under vacuum for 2 h (Ru-MOF_{ht}). Elemental analysis for Ru-MOF_{ht}, % obs.: C: 27.6; H: 1.7, is consistent with assigned $[\text{Ru}_3(\text{btc})_2\text{X}_x\text{Y}_{1.5-x}]$ (where X, Y = Cl⁻ or OH⁻) molecular formula.

Alternative synthetic procedure for the reference sample (Ru-MOF) preparation using $[\text{Ru}_2(\text{CH}_3\text{COO})_4\text{Cl}]$: The same experimental conditions as described before were used. A reaction mixture of the composition $1.5[\text{Ru}_2(\text{CH}_3\text{COO})_4\text{Cl}] : 2\text{H}_3\text{btc} : 5\text{CH}_3\text{COOH} : 925\text{H}_2\text{O}$ was heated at 160°C for 72 h in a Teflon-lined autoclave. After cooling to room temperature, a deep green product was collected with a membrane filter, washed with water and dried at room temperature. The PXRD and FTIR data of the product are identical to those observed before for the Ru-MOF material synthesized directly from $\text{RuCl}_3 \times x\text{H}_2\text{O}$ (**Fig. S12**).

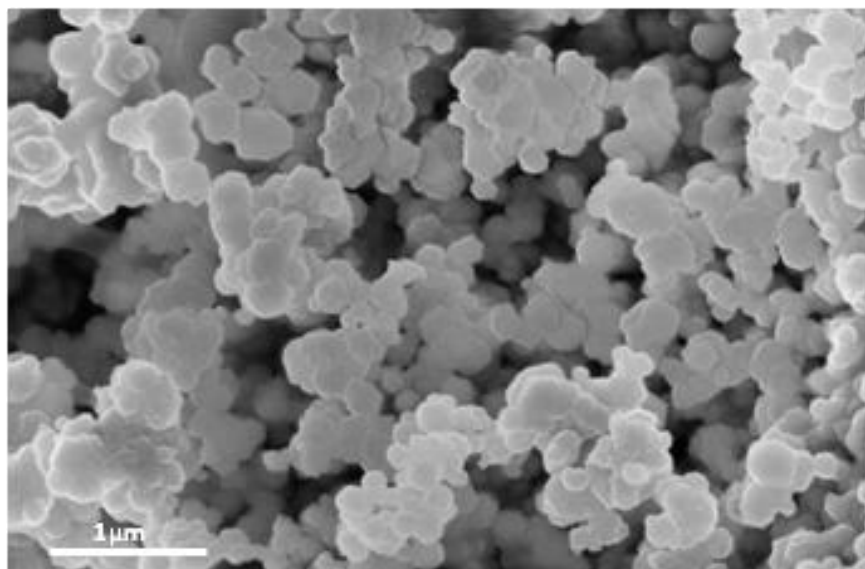


Figure S1 SEM image of Ru-MOF_{as} powder sample.

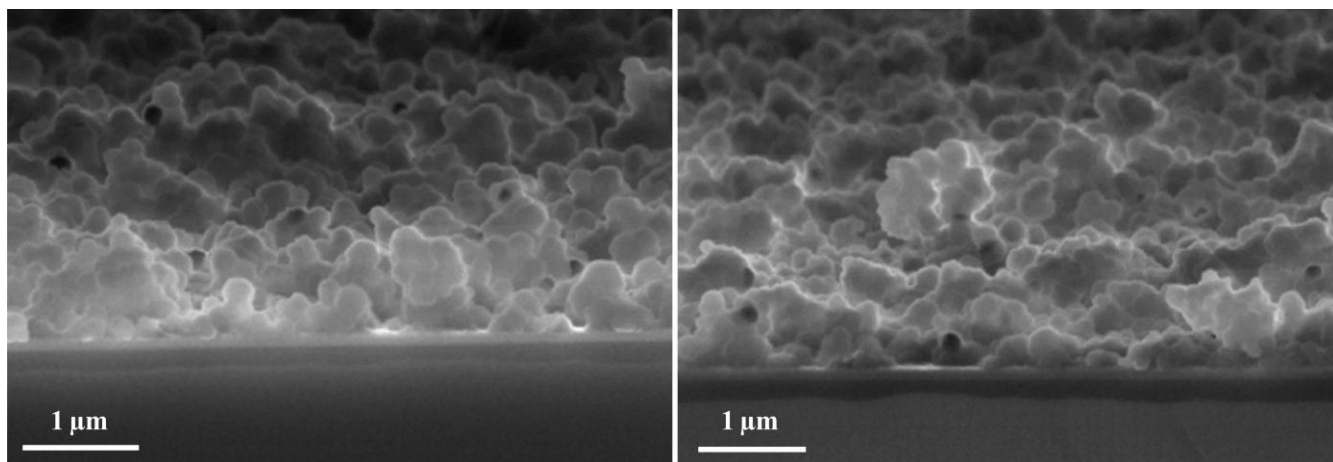


Figure S2 Cross-section SEM images of Ru-MOF thin films grown on Al₂O₃ (left) and SiO₂ (right) surfaces.

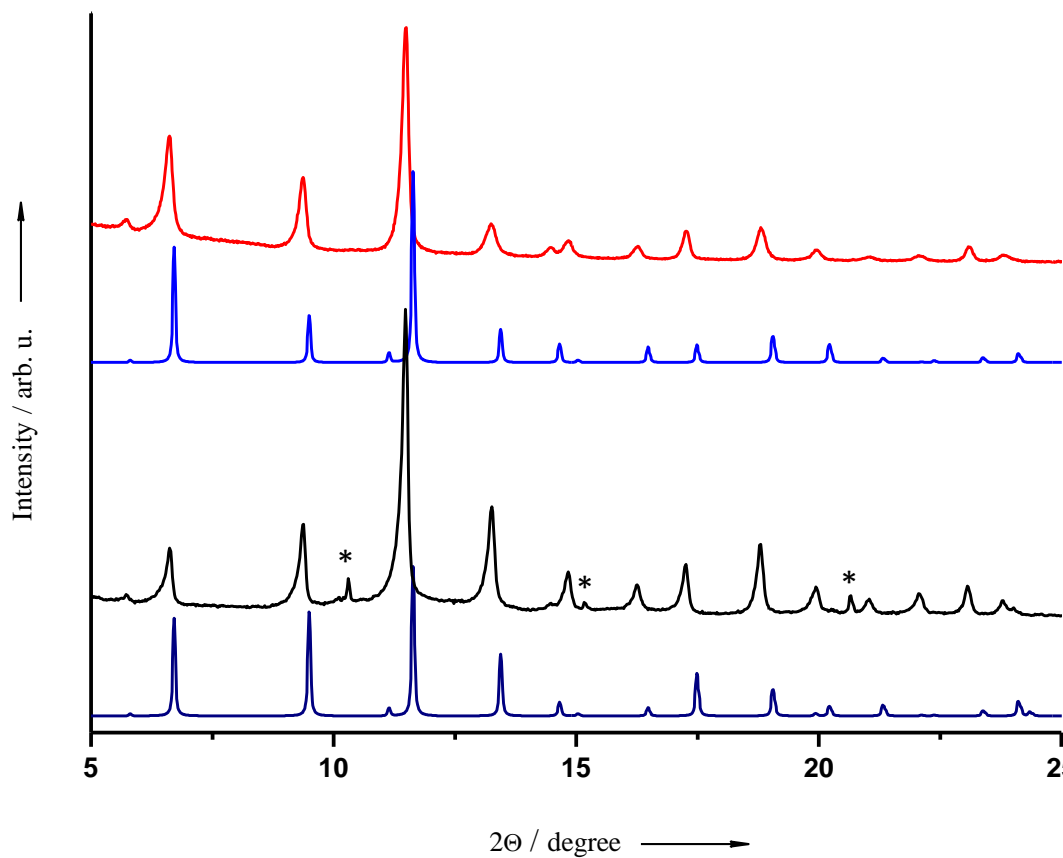


Figure S3 Comparison of the PXRD patterns of **Ru-MOF_as** (black line; signals marked with asterisks are present due to traces of H₃btc) and **Ru-MOF_ht** (red line) materials with simulated powder patterns of the crystal structure of **[Cu₃(btc)₂]_{as}** (dark blue line) and **[Cu₃(btc)₂]_{ht}** (bright blue line), respectively.

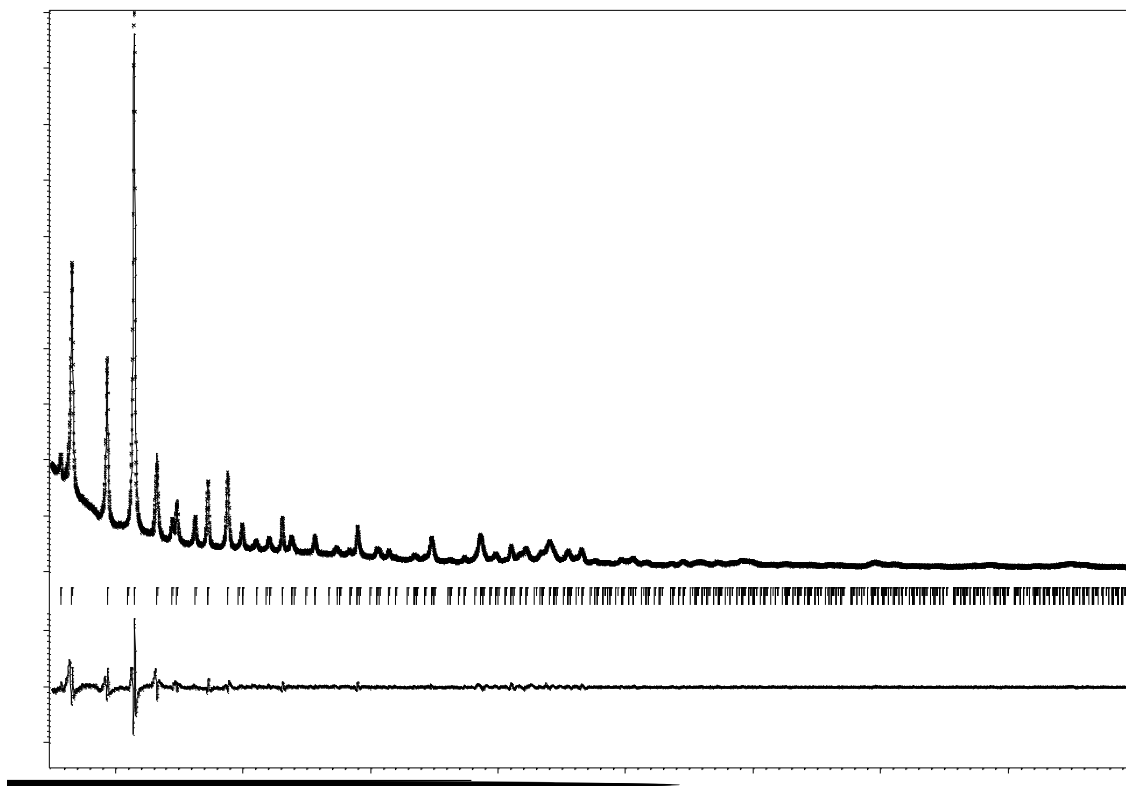


Figure S4 PXRD data of Ru-MOF_ht. Least-squares cell-parameters and line-profile refinement ($a = 26.634(2) \text{ \AA}$, $V = 18893.7(1) \text{ \AA}^3$, $R_p = 4.74$, $R_{wp} = 6.29$).

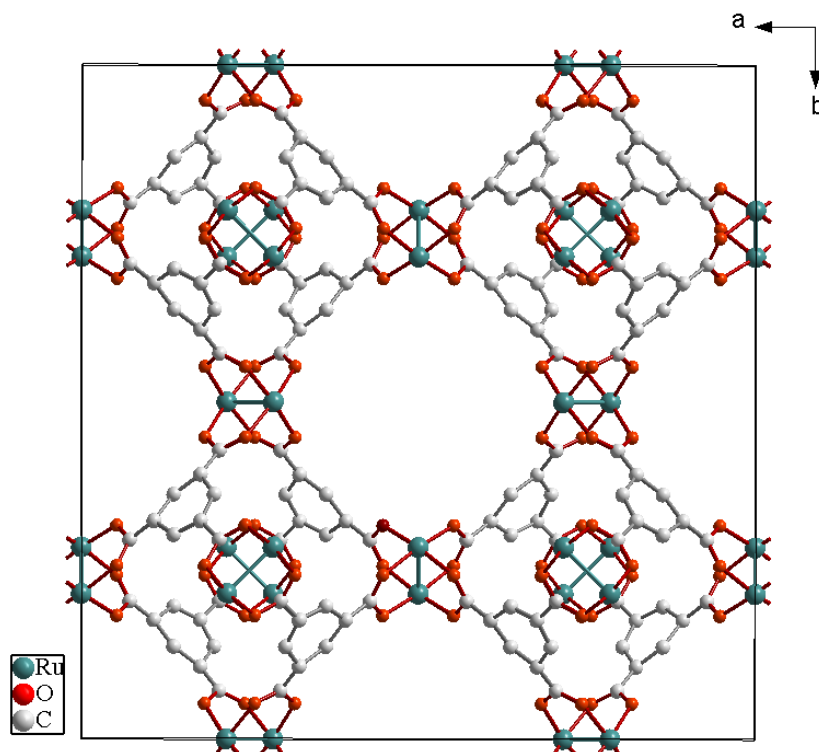


Figure S5. Unit cell view along *c*-axis. Crystal structure has been refined using the atomic coordinates, interatomic and angle restrains published for the $[\text{Cu}_3(\text{btc})_2]_{\text{ht}}$ crystal structure.³ Finally, the obtained model was refined by the Rietveld method with Jana2000 software.⁴ Isotropic parameters values (*U*_{iso}) were fixed as 0.038 \AA^{-2} for all atoms. The next parameters were refined step by step: (i) zero shift, background's function, profile (pseudo-Voigt function) and cell parameters; (ii) structural parameters; (iii) all parameters together to give the final R_p , R_{wp} , R_f , R_{fw} and R_B factors. Ru...Ru distances in dimmers (2.60 \AA) are a bit longer, then found in known $\text{Ru}_2^{\text{II,III}}$ carboxylate compounds ($2.29\text{--}2.43 \text{ \AA}$).⁵

Table S1. Coordinates of the atoms in Ru-MOF structure.

Atom	x/a	y/b	z/c
Ru	0.2154	0.2154	0
O	0.1830(3)	0.2571(4)	-0.0525(5)
C1	0.1765(5)	0.3235(5)	-0.1075(9)
C2	0.2045(3)	0.2955(3)	-0.0717(5)
C3	0.1969(9)	0.3630(8)	-0.1370(8)

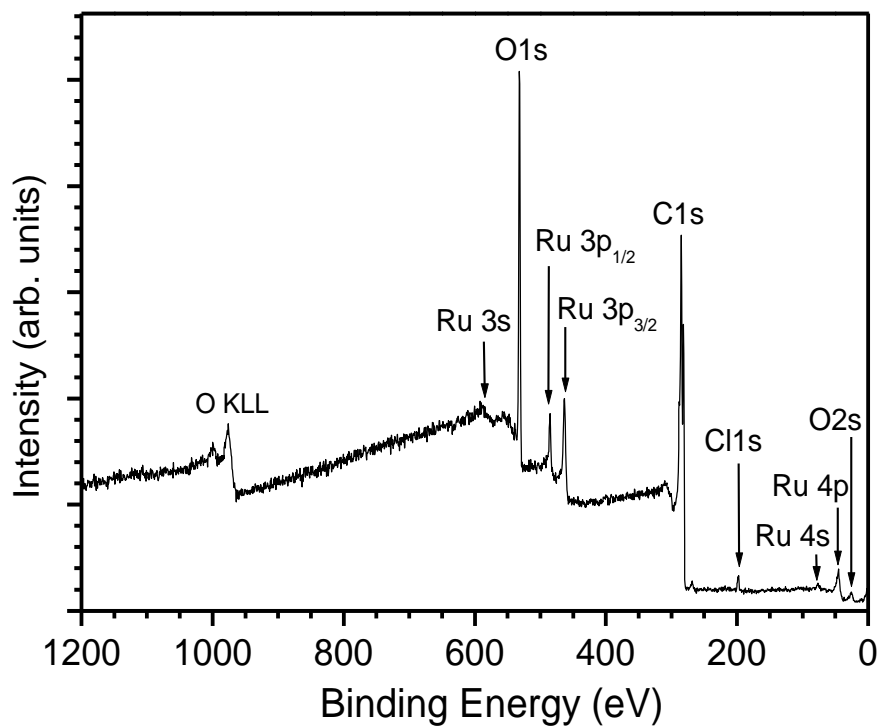


Figure S6 XP survey spectra of the Ru-MOF sample.

As shown in **Figure S6** ruthenium, chlorine, oxygen- and carbon-related peaks are detected in the XP survey spectra obtained for Ru-MOF sample.

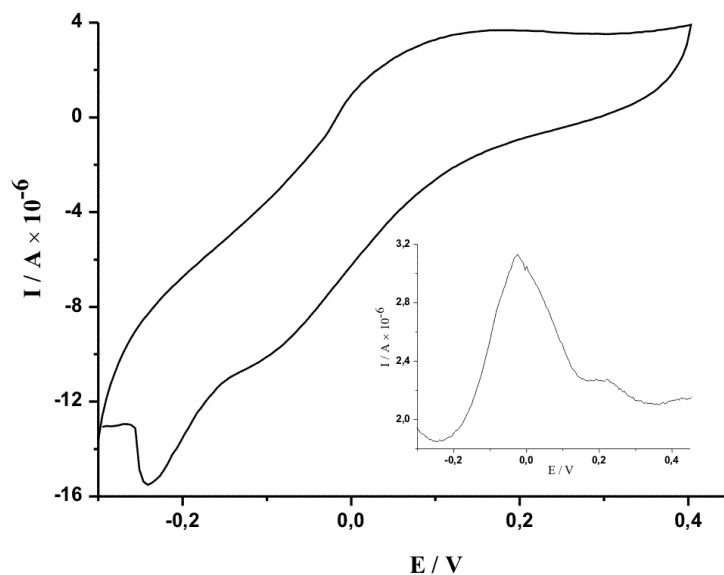


Figure S7 Cyclic voltammetry and differential pulse voltammetry (insert) of Ru-MOF.

Open circuit potential of the Ru-MOF sample was 0.325 V.

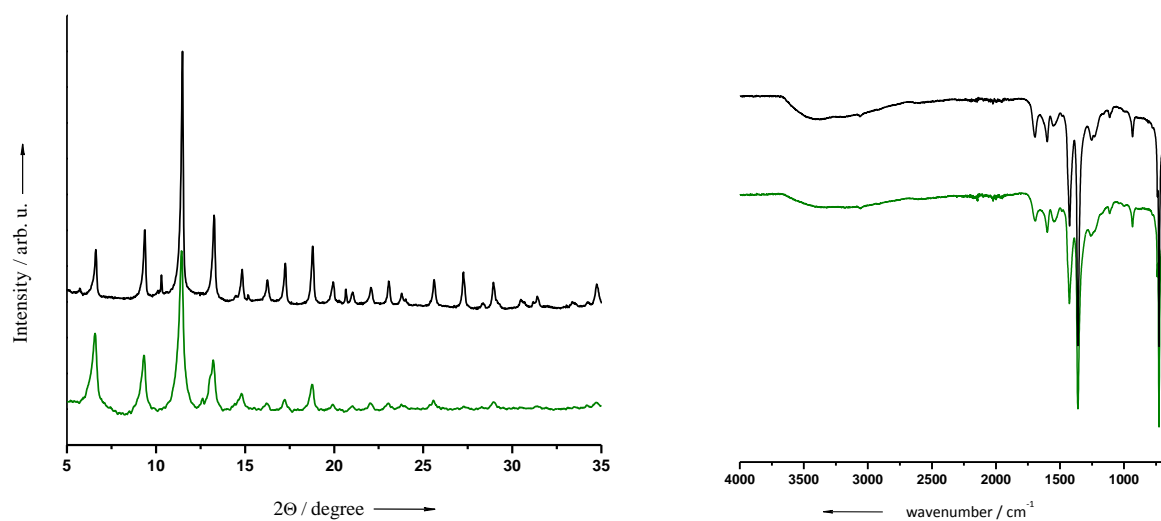


Figure S8 Comparison of the PXRD patterns (left) and FTIR spectra (right) of Ru-MOF_{as} samples obtained using $\text{RuCl}_3 \times \text{H}_2\text{O}$ (black lines) and $\text{Ru}_2[\text{CH}_3\text{COO}]_4\text{Cl}$ (green lines) as a metal precursors.

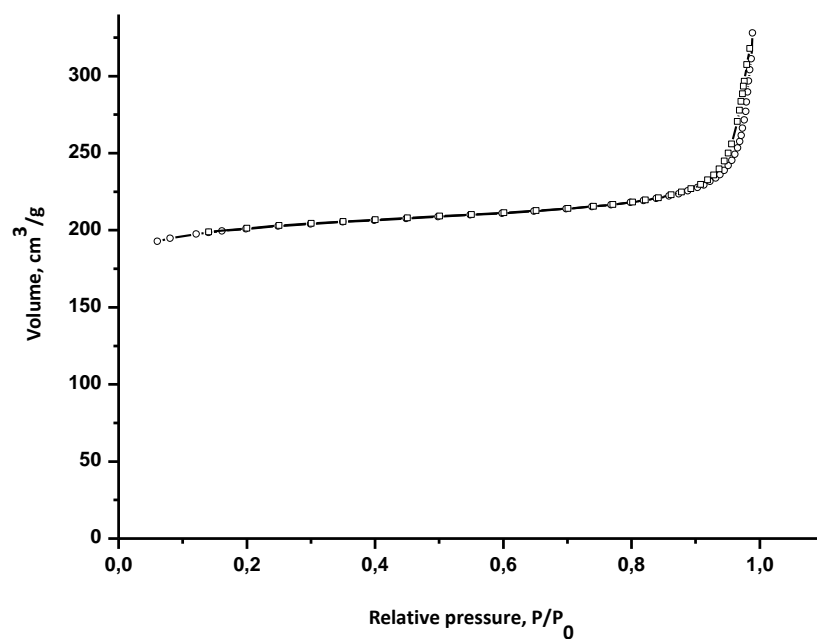


Figure S9 N_2 adsorption isotherm on Ru-MOF at 77.35K (P_0 – saturation pressure; \square – adsorption, \circ – desorption)

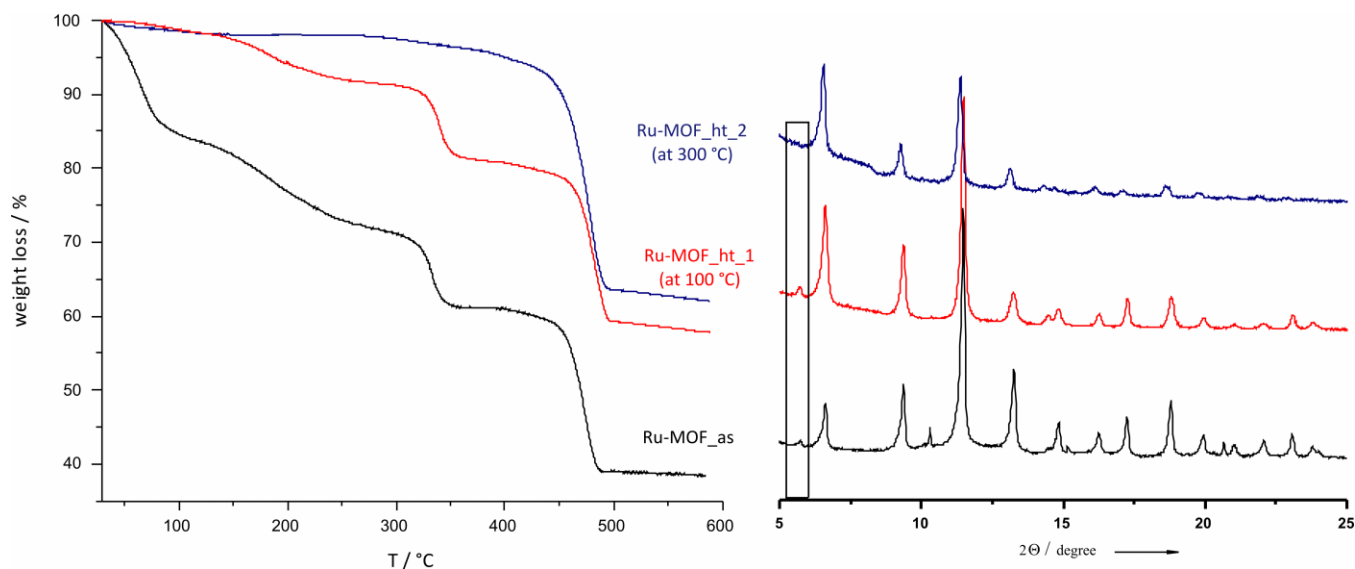


Figure S10 Thermal gravimetric (TG) curves (left) and respective powder X-ray diffractions (right) of **Ru-MOF_as** (black lines), **Ru-MOF_ht_1** (calcinated at 100 °C under vacuum – red lines) and **Ru-MOF_ht_2** (calcinated at 300 °C under vacuum – blue lines).

Analyzing the TG curves of as-synthesized (**Ru-MOF_as** – black line) and calcinated (**Ru-MOF_ht** – red line) materials we can conclude that the weight loss steps observed in-between 25 and 200 °C are due to desorption of the solvent H₂O. At higher temperatures for both **Ru-MOF_as** and **Ru-MOF_ht_1** samples two more steps are observed (around 300 and 450 °C). In order to determine the decomposition temperature of the framework addition experiment has been conducted: **Ru-MOF_as** has been calcinated at 300 °C under vacuum (**Ru-MOF_ht_2**). The comparison of powder X-ray diffractions data of **Ru-MOF_as**, **Ru-MOF_ht_1** (calcinated at 100 °C) and **Ru-MOF_ht_2** (calcinated at 300 °C) reveals that around 300 °C the framework most probably partly decomposes. The powder diffractogram of **Ru-MOF_ht_2** still contains peaks positions of which are in good correlation with those of **Ru-MOF_as** and **Ru-MOF_ht_1**. However, the first line at 5.7° (2θ) which is characteristic for **Ru-MOF_as** and **Ru-MOF_ht_1** samples could not be observed any more in case of **Ru-MOF_ht_2** (marked part on the picture). In addition the ratio of the line intensities of **Ru-MOF_ht_2** also changes. Thus, the thermal behavior of Ru-MOF is more complicated than of HKUST-1³ and for more information additional experimental studies are required (for example, the determination of the species with mass-spectrometry as it was done in [Mo₃(btc)₂]⁶ case).

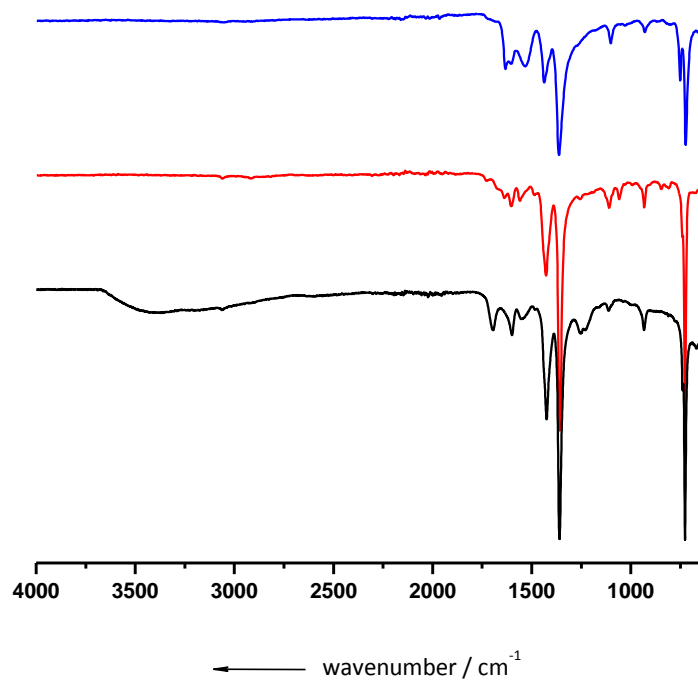


Figure S11 Comparison of the FTIR spectra of **Ru-MOF_{as}** (black line), **Ru-MOF_{ht}** (red line) and **[Cu₃(btc)₂]_{ht}** (blue line) materials.

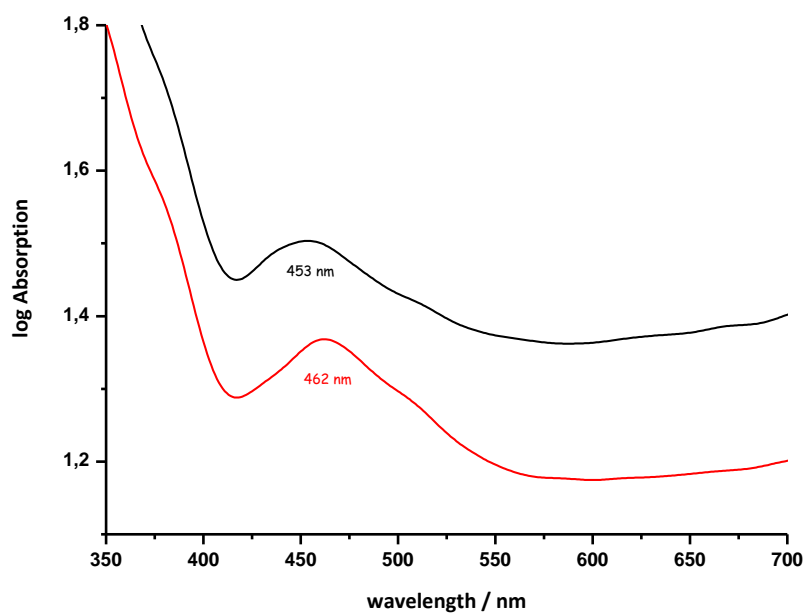


Figure S12 UV/VIS spectra of **Ru-MOF_{as}** (black line) and **Ru-MOF_{ht}** (red line).

References:

1. R. W. Mitchell, A. Spenser and G. Wilkinson, *J. Chem. Soc., Dalton Trans.*, 1973, 846; G. Ribeiro, F. M. Vichi, D. de Oliveira Silva, *J. Molec. Struct.*, 2008, **890**, 209.
2. The program package JulX was used for spin-Hamiltonian simulations and fittings of the data by a full-matrix diagonalization approach (E. Bill, unpublished results).
3. S. S.-Y. Chui, S. M.-F. Lo, J. P. H. Charmant, A. G. Orpen and I. D. Williams, *Science*, 1999, **283**, 1148.
4. Petříček, V., Dušek, M., Palatinus, L. Jana2000. The crystallographic computing system. 2000, <http://www-xray.fzu.cz/jana/Jana2000/jana.html>.
5. Carlos A. Murillo, "Multiple Bonds Between Metal Atoms" (Eds.: F. A. Cotton, C. A. Murillo and R. A. Walton), Springer Science and Business Media, Inc., New York, 2005, chapter 9 "Ruthenium Compounds" (written by P. Angaridis), pp 377-430.
6. M. Kramer, U. Schwarz and S. Kaskel, *J. Mater. Chem.*, 2006, **16**, 2245.